Augmentation of integrin-mediated mechanotransduction by hyaluronic acid

Anant Chopra[1,3], **Maria E. Murray**[3,4], **Fitzroy Byfield**[4], **Melissa Mendez**[4], **Ran Halleluyan**[2], **David Restle**[3,4], **Dikla Raz-Ben Aroush**[4], **Peter A. Galie**[4], **Katarzyna Pogoda**[4,5], **Robert Bucki**[4], **Cezary Marcinkiewicz**[6], **Glenn D. Prestwich**[7], **Thomas Zarembinski**[7], **Christopher S. Chen**[3,4], **Ellen Puré**[8], **J. Yasha Kresh**[1,2], and **Paul A. Janmey**[4]

[1]Dept. of Cardiothoracic Surgery, Drexel Univ. College of Med, Philadelphia, PA [2]Dept. of Medicine, Drexel Univ. College of Med, Philadelphia, PA [3]Dept. of Bioengineering, Univ. of Pennsylvania, Philadelphia, PA [4]Institute for Medicine and Engineering, Univ. of Pennsylvania, Philadelphia, PA [5]The Henryk Niewodniczański Institute of Nuclear Physics, Kraków, Poland [6]Dept. of Biology, Temple University, Philadelphia, Pennsylvania [7]Glycosan Biosystems, Salt Lake City, UT [8]Dept. of Animal Biology, School of Veterinary Medicine, University of Pennsylvania, Philadelphia, PA

Abstract

Changes in tissue and organ stiffness occur during development and are frequently symptoms of disease. Many cell types respond to the stiffness of substrates and neighboring cells in vitro and most cell types increase adherent area on stiffer substrates that are coated with ligands for integrins or cadherins. In vivo cells engage their extracellular matrix (ECM) by multiple mechanosensitive adhesion complexes and other surface receptors that potentially modify the mechanical signals transduced at the cell/ECM interface. Here we show that hyaluronic acid (also called hyaluronan or HA), a soft polymeric glycosaminoglycan matrix component prominent in embryonic tissue and upregulated during multiple pathologic states, augments or overrides mechanical signaling by some classes of integrins to produce a cellular phenotype otherwise observed only on very rigid substrates. The spread morphology of cells on soft HA-fibronectin coated substrates, characterized by formation of large actin bundles resembling stress fibers and large focal adhesions resembles that of cells on rigid substrates, but is activated by different signals and does not require or cause activation of the transcriptional regulator YAP. The fact that HA production is tightly regulated during development and injury and frequently upregulated in cancers characterized by uncontrolled growth and cell movement suggests that the interaction of signaling between HA receptors and specific integrins might be an important element in mechanical control of development and homeostasis.

Keywords

Hyaluronan; Hyaluronic Acid; Mechanosensing; Yes Associated Protein (YAP); Traction stresses; Cell spreading; Extracellular matrix

---

Correspondence to: J. Yasha Kresh; Paul A. Janmey.

1.0. Introduction

Changes in tissue and organ stiffness are frequently symptoms of diseases such as cancer [1], liver fibrosis [2], and atherosclerosis [3], and these physical changes have been suggested to contribute to and not only be symptoms of the disease. For example, liver stiffness, as quantified by its shear modulus, increases during experimentally-triggered liver fibrosis prior to increased matrix deposition or altered cell morphology [4] by a mechanism involving lysyl oxidase [5]. Similarly, the development of atherosclerotic lesions in an apoE null mouse model can be reversed by inhibition of abnormal lysyl oxidase activity and subsequent reversal of arterial stiffening [3]. Such results suggest that changes in tissue mechanics that can activate hepatic stellate cells [6], portal fibroblasts [7] or vascular smooth muscle cells [8] in the affected organs precede and therefore might cause or at least contribute to development of the pathologic state. The response of cells to abnormal matrix stiffness can also render them resistant to chemotherapeutic agents, possibly because of the changes in the cytoskeleton-membrane interface [9]. Such effects in vivo have motivated studies in vitro to determine how physical properties such as increased cellular tension or adherence to substrates of differing stiffness affect cell function under conditions where physical stimuli can be isolated from biochemical signals.

Many cell types alter their structure and function in vitro depending on the mechanical properties of the materials to which they adhere [10] and on the type of adhesion receptor by which they bind [11–13]. Most studies of cellular mechanosensing have used inert, non-adhesive, soft materials for which mechanical properties can be controlled, and coupled these substrates to cell adhesion proteins or synthetic ligands that engage specific transmembrane proteins. Independent control of mechanical and adhesive changes in the substrates has been essential to demonstrate that changes in substrate viscoelasticity *per se*, and not a coincident change in cell signaling caused by altered adhesion protein presentation causes the change in phenotype. The large majority of mechanosensing studies have used the integrin ligands fibronectin, collagen, laminin, or RGD-containing peptides as the adhesive anchor, and often polyacrylamide or other hydrogels such as alginate, poly(ethylene glycol) or methacrylated hyaluronan to produce substrates softer than 50 kPa. A smaller but growing number of studies have investigated mechanosensing mediated by cadherins to mimic cell-cell junctions [13, 14].

Studies in vitro of cells anchored to substrates through integrins or in some cases cadherins, show that a common, though not universal, response of cells to substrate stiffness is an increase in adherent area, increased traction forces applied to the substrate, assembly of large actin bundles called stress fibers, and activation of signaling intermediates such as small GTPases and tyrosine kinase pathways that regulate actin assembly and acto-myosin contractility [15, 16]. The inference from such studies is that most cell types actively probe the mechanics of their environment by acto-myosin dependent forces, which increase when the resistance imposed by the substrate increases, and the feedback between cell and substrate reorganizes the cytoskeleton to achieve a homeostatic state appropriate for each physical context [17]. Substrate stiffness and the resulting increase in cell-generated forces can also increase activity of matrix-bound growth factors such as TGF-beta, that further increase development of the phenotype associated with growth of stiff substrates [18].

Response to substrate stiffness is highly cell-type specific, and neurons for example, have a unique response to stiffness, in which matrix stiffness greater than that of the normal CNS tissue inhibits neurite outgrowth and growth cone spreading [19–21]. Myocytes have a particularly striking and well-documented response to matrix stiffness, with a distinct optimum for development of sarcomeres and an elongated shape that depends on both matrix stiffness [22–24] and the type of adhesion receptor [13, 14, 25]. On polyacrylamide

(PAA) gels that are laminated with ligands for integrins, cardiac myocytes develop well organized sarcomeres only when cultured on substrates with elastic moduli in the range of 10 kPa to 30 kPa, near those of the healthy tissue. On stiffer substrates (>60 kPa) approximating the damaged heart, myocytes form stress fiber-like filament bundles but lack organized sarcomeres or an elongated shape. On soft (<1 kPa) PAA gels myocytes exhibit disorganized actin networks and sarcomeres. On N-cadherin-coated PAA gels, the response is similar but the optimum is shifted to slightly lower stiffness (5 kPa) [14].

In contrast to the simplified chemical composition of soft substrates used for mechanosensing studies in vitro, cells engage their extracellular matrix (ECM) in vivo both by mechanosensitive adhesion complexes and by other surface receptors for ECM components that cannot act as adhesive anchors, but that potentially modify the mechanical signals transduced at the cell/ECM interface. Such ECM components include not only growth factors such as TGF-beta but also proteoglycans and glycosaminoglycans such as hyaluronic acid that constitute a major fraction of the total ECM content, and that change in abundance during development, wound healing, and disease. For example, during development, cardiac myocytes assemble and organize their internal structures within a complex mechanical tissue environment bounded by an especially soft (E ~ 20–100 Pa) [26, 27] hyaluronan-and fibronectin-containing cardiac jelly and a considerably stiffer (E~10kPa) [23] compacted myocardial tissue. How a sarcomere forms in such a soft matrix in vivo, whereas a substrate with the same low elastic modulus prevents sarcomere formation in vitro is not known, but the transient expression of hyaluronic acid during conditions where cells mature within a very soft matrix suggests that it might contribute to the development of cell morphology in a manner that is not fully reproduced by integrin signaling alone.

Hyaluronic acid (HA) is a high molecular weight (6–7000 kDa), linear polysaccharide found in soft tissue and synovial fluid that consists of N-acetyl-D-glucosamine and D-glucuronic acid residues that give the molecule a highly negative charge. HA interacts with cells through its receptors CD44 [28], RHAMM [29], layilin [30] and ICAM-1 [31]. HA can also bind fibronectin (Fn) [32] and collagen VI [33] in vitro, suggesting that HA might modify cell adhesion to these integrin ligands. HA is synthesized by many cell types and either retained on the cell surface as a pericellular coat or cleaved from the cell and released into the extracellular matrix (ECM) [34]. HA and HA receptor syntheses are tightly regulated during development [35] and often activated during normal wound healing, especially during fetal wound repair that enables healing without scarring [36]. HA in either soluble or crosslinked forms is a commonly used simple and semi-synthetic soft material with numerous current clinical applications [37], although usually in a form that is highly modified by methacrylation or other covalent linkages that might affect its binding to HA receptors. The studies in this report test the hypothesis that the presence of long unmodified hyaluronan polymers within a matrix that also contains integrin ligands such as fibronectin alters the mechanosensing signals mediated by the activated integrin to elicit a phenotype that cannot be attained under the same mechanical conditions by integrin engagement alone.

2.0. Materials and methods

2.1. Cell line culture and/or isolation

Neonatal ventricular rat myocytes (NVRM) were harvested from the hearts of 1- to 3-day-old euthanized Sprague-Dawley rat pups using a cell isolation kit (Cellutron Life Technology, Baltimore, MD) as described previously[14]. Isolated cardiac myocytes were pre-plated for 1 to 2 h to purify the myocyte population. The cells were cultured at a density of 7,000 cells/cm^2 in high serum (10% fetal bovine serum) medium (Cellutron) on the various gel substrates for 24 h. The medium was changed to low serum (2% fetal bovine serum) and maintained for another 24 h. This time period proved sufficient to allow the cells

to attach and spread completely after the isolation procedure. Human mesenchymal stem cells (hMSCs) (Lonza), 3T3 fibroblasts and human umbilical vein endothelial cells (HUVECs) were cultured in their respective medium for a period of 24 hours or greater.

2.2. Hydrogel substrate preparation

Polyacrylamide (PAA) and hyaluronan gels of desired stiffness were made using methods described elsewhere [10, 12, 14]. Briefly, the acrylamide solutions (Bio-Rad Laboratories, Hercules, CA) are polymerized using TEMED (Fisher BioReagents, Fairlawn NJ) and 10% ammonium persulfate (Fisher BioReagents). The solution was deposited on a 20-mm square glass coverslip pretreated with 3-aminopropyltrimethoxysilane (Sigma-Aldrich, St. Louis, MO) and 0.5% glutaraldehyde (Sigma-Aldrich). The gels were coated with 0.1mg/ml of bovine fibronectin (Fn) (Sigma-Aldrich) through the cross-linker N-Sulfosuccinimidyl-6-(4′-azido-2′-nitrophenylamino) hexanoate (0.5 mg/ml in 50 mM HEPES buffer pH 8) (Thermo Fisher Scientific, Waltham, MA).

Semi-synthetic hyaluronan based hydrogels (HyStem, Glycosan BioSystems) were prepared by reacting the thiol-modified HA (HyStem) with poly(ethyleneglycol) diacrylate (PEGDA Mw=3400 Da, Extralink, Glycosan BioSystems). The hydrogels were formed in combination with fibronectin or any other protein of choice. Modification of these proteins to covalently link them throughout the hydrogel network was performed using Maleimide-dPEG8-N-HydroxySuccinimide ester (M-dPEG-NHS, Quanta BioDesign). Briefly, HyStem was dissolved with degassed water (DG Water, Glycosan BioSystems) to result in a final gel concentration of 0.8 wt %. The protein was activated by reacting in 1:10 (wt/wt) ratio with the M-dPEG-NHS in a sterile aqueous solution for 30 minutes. This solution was then added to the previously dissolved HyStem, allowed to react for an additional 30 minutes, and finally crosslinked with Extralink using a 1vol:4vol Extralink to HyStem ratio. Protein concentrations varied between 5 μg/mL up to 1 mg/mL and Extralink concentrations varied between 5 mg/mL up to 40 mg/mL. The stiffest hydrogels were prepared using poly(ethyleneglycol) tetra-acrylate (4-arm acrylated PEG, Mw 10,000 Da) at 40 mg/mL. Fibronectin has been reported to bind directly to hyaluronan [32], for that reason unmodified fibronectin was added to the HA solution and crosslinked with PEGDA. No discernible differences in cell spreading were observed. Ligand density on the surface of the hydrogels was quantified using a previously established method[14, 38]. Briefly, CY5-labeled fibronectin was incorporated in the HA gels and coated on the PAA gels. The gel surface was visualized using confocal microscopy (Olympus). The fluorescence intensity on the surface of the hydrogels was quantified. Five random images of each gel surface were taken, analyzed, and averaged. The intensity of the unlabeled gels, which represents autofluorescence, was subtracted from the average intensity of the labeled gels.

2.3. Quasi 3D and 3D culture System

Substrates were sandwiched in order to mimic a three-dimensional (3D) tissue culture system as described previously, with minor modification [38]. hMSCs were plated on a 22-mm gel and allowed to spread overnight. Culture medium was removed and a second coverslip coated with a hyaluronic acid gel was inverted on top of the cells. In order to bring the cells in close proximity with the second coverslip, a 30 g weight was placed on top of the sandwich for 30 seconds. Medium was then added around the weight, and then the weight was removed. Cells were imaged with phase microscopy after 24 hours.

Myocytes and support cells (fibroblasts) were isolated from neonatal rat cardiac tissue as described previously. Cells were directly suspended in NaOH neutralized solution of 1 mg/mL fibrin, 0.25 mg/mL collagen-I, 1X medium and varying concentrations of HA. The cell and ECM solution (0.5ml) was allowed to polymerize at 37°C for 30 minutes in 24 well

plates. Images of constructs at the specified time points were taken to calculate volume to compute compaction. To determine construct stiffness, constructs were tested in uniaxial, unconfined compression at a uniform strain rate of 10%/sec. Elastic modulus was calculated by taking the slope of the stress-strain curve at a linear region from 5–10% strain to assure that the small strain assumption was valid.

2.4. Micropatterning of hyaluronan gels for traction force microscopy

Micropatterning of soft hyaluronan gels was done through an indirect micro-contact procedure developed in the laboratory. Polydimethylsiloxane (PDMS) stamps of 1µm dot patterns for microcontact printing were generously provided by Dr. Erdem Tabdanov, Columbia University. These patterned stamps were inked with a 5:1 mixture of DPEG8 modified fibronectin and CY5 conjugated fibronectin. The inked PDMS stamps were stamped onto a clean 20mm glass coverslip. Hyaluronan and crosslinker PEG-TA/DA were deposited onto a hydrophilic glass substrate. The patterned glass surface was then placed on top of the HA solution and the HA solution was allowed to polymerize for a period of 1 hour. This method allowed the imprinting of fibronectin micropatterns covalently to the HA gel. The top coverslip was removed carefully and the patterned gel was washed thoroughly with 1XPBS before plating cells. The patterns were checked for uniformity using immunofluorescence.

2.5. Live cell imaging

Fn-HA or Fn-PAA gels were made on coverglasses in 60mm petri dishes drilled with an 18mm hole in the center of the bottom to which a coverless was glued (Sylgard 184; Dow Corning) to the underside. Mouse embryonic fibroblasts (MEFs) were collected following trypsinization and pipetted into a dish containing a gel and incubating in a humid chamber at 37 °C and 5% CO_2 (Tokai Hit) such that the cells would settle without contacting one another. Images were then collected every minute. Image series were collected at multiple points using a motorized stage (ASI; MS-2000) mounted on a Leica widefield microscope at 10×. The cell perimeter was then traced (ImageJ) each minute and perimeter lengths used to ascertain the onset and rate of cell spreading.

2.6. Immunofluorescence and morphological studies

Cells were fixed with 4% paraformaldehyde (Sigma) for 10 min at room temperature, permeabilized with 0.1% Triton X-100 in TBS for 10 min, and then. Incubated for 1 h with primary antibodies directed against anti-alpha actinin (1:400; Sigma), paxillin (Sigma)or YAP (H-9, Santa Cruz). Secondary antibodies included Alexa 488 or 568 (Invitrogen). For some experiments, cells were incubated with phalloidin–tetramethylrhodamine B isothiocyanate (1 µg/ml; Sigma) or bisbenzimide (1 µg/ml; Sigma). Focal adhesions were visualized following transfection with GFP-paxillin.

The cells were imaged using a conventional microscope (Carl Zeiss, Thornwood, NY) at ×20 and ×63 using a proprietary software (Axiovision; Carl Zeiss). Cell area was computed using a dedicated MATLAB program (The MathWorks, Natick, MA) that quantifies (in pixel intensity units) the contrast between the fluorescent cells and the dark background. For each image, the degree of contrast at the cell border was defined and outlined by an unbiased observer.

2.7. Cell proliferation assay

hMSCs were cultured on various substrates at low densities and imaged at low magnification every several days. The number of cells per field of view were counted and averaged. 3T3 or HUVEC cells were sub-cultured onto various substrates at low densities.

At least three times over the subsequent 24 hours, the number of cells in many fields of view were counted at low magnification. Population doubling times were calculated by fitting an exponential growth equation (GraphPad Prism; GraphPad Software) to the average number of cells per field over time.

2.8. Atomic force microscopy

3T3 fibroblasts were plated on HA-Fn gels (0.8% HA, 0.1mg/ml FN) prepared on top of CELLocate coverslips (square size 55 um) and allowed to spread for 24 hrs. AFM measurements were conducted at room temperature using a Bioscope DAFMLN-AM head(Veeco, Woodbury, NY) mounted on an Axiovert 100 microscope (Zeiss, Thornwood, NY). A silicon nitride cantilever (196 μm long, 23 μm wide, 0.6 μm thick, 0.06 N/m spring constant) with a bead tip (3.5 μm in diameter) was used for indentation. Cells were indented at 3 areas between the nucleus and the cell edge (red dots, top left image) and 3 areas of the HA-Fn gel within 30 μm of the cell edge (blue dots, top left image). Images were taken of each cell measured by AFM. Samples were then placed in Ca^+/Mg^+ free PBS at 37°C for 30 mins then gently rinsed until cell detachment was observed. Areas of the HA-Fn gel to which cells were previously attached were located using grid coordinates from previously taken images and indented (blue dots, top right image). To calculate the Young's modulus, the first 500–800 nm of tip deflection were fit to the Hertz model for a sphere making contact with a homogenous elastic half-space

$$f_{bead} = k * d_{cantilever} = \frac{4}{3} \frac{E}{1-v^2} \sqrt{R\delta^{\frac{3}{2}}}$$

where f_{bead} is the force on the bead, $d_{cantilever}$ is the deflection of the cantilever measured by the AFM, E is the Young's modulus, v is the Pvggoisson ratio, R is the radius of the bead, and δ is the vertical displacement of the cantilever

2.9. Traction force microscopy

Traction forces were found as previously described [39, 40]. Cells were cultured for 24 hours on fibronectin dot grid patterned 300Pa HA gels. Traction stresses were estimated by measuring the dot displacement vectors using a custom written Matlab software (The MathWorks, Natick, MA) used for detecting displacements of PDMS posts [41]. A threshold displacement of 0.6 pixels was taken from a null image of patterned dots (without cells), to account for any patterning error. The corresponding traction stress (T) vector for each dot was calculated assuming a uniform tangential traction stress distribution over a circular area on an isotropic elastic half space as described previously[42].

$$T = \frac{2\pi Gau}{2-\gamma}$$

where G is shear modulus of the substrate, a is the area of the dot and u is the displacement vector. The resting traction stresses exerted by myocytes on Fn coated PAA and HA substrates of 300 Pa rigidity were computed by measuring the displacement of 0.2 μm fluorescent beads (Molecular Probes, Invitrogen) embedded within the gels as described previously [39, 40]. Briefly, images of bead motion near the substrate surface, distributed in and around the contact region of a single cell (before and after cell detachment with 0.5% trypsin EDTA), were acquired (Zeiss Observer Z1 Microscope), aligned using Image J (National Institutes of Health, Bethesda, MD) and converted into displacement vectors using

the particle image velocimetry program implemented through the Image J plugin. An estimate of cell traction stresses were computed from the substrate displacement fields using the Fourier transform traction cytometry (FTTC) method, the code for which was obtained as an image J plugin (https://sites.google.com/site/qingzongtseng/piv) and is described elsewhere [39].

2.10. Statistical analysis

Two-tailed t-test was used to determine statistical significance and analysis of variance was determined by ANOVA (α value of 0.05 was considered significant).

3.0. Results

3.1. Muscle and non-muscle cell spreading, stress fiber and focal adhesion assembly on soft HA-Fn gels

Figure 1 shows human bone marrow-derived mesenchymal stem cells (hMSCs), rat cardiac myocytes, rat cardiac fibroblasts, human umbilical vein endothelial cells (HUVECs), and NIH-3T3 fibroblasts on soft gels with shear moduli between 200 and 300 Pa, formed by either crosslinked HA or polyacrylamide (PAA) and covalently modified with fibronectin (Fn). On PAA, an inert linearly elastic hydrogel, cells attached through Fn-binding integrins, but they did not spread or develop the large actin assemblies (Fig. 1b, e, h, k, n) as observed for cells on rigid substrates (Fig. 1c, f, i, l, o). However, when HA rather than PAA forms the matrix, all five cell types develop large adherent areas, actin bundles (Fig. 1a, d, g, j, m) and FAs (Fig. 1m inset) equivalent to those formed on rigid PAA or glass. Cells subcultured in serum-containing medium on micropatterned Fn islands on HA gel surfaces adhere only to the Fn islands despite the availability of enough soluble Fn in the serum to saturate the gel by adsorption (Supplemental Fig. 1). Therefore HA behaves similar to a non-adhesive inert substrate like PAA. Remarkably, cells on HA substrates were able to cluster integrins to an extent similar to that observed on stiff 30 kPa PAA substrates (see arrows, Supplementary Fig. 1). These results correlate well with the observed focal adhesion size on HA, suggesting that signals mediated through HA receptors can enhance integrin clustering, which has largely been shown to be an adhesion and cytoskeleton force driven response [43].

3.2. Cell spread area and rate at low Fn ligand densities

Figure 2A shows that the spreading of cells on HA-Fn gels depends on the amount of Fn incorporated in the matrix, and that similar spreading did not occur on PAA gels despite the 100 fold increase in Fn concentration. Since the concentration of fibronectin incorporated throughout the HA gels is the same as that crosslinked to the surface of PAA gels, the quantified density of Fn on the HA surface was relatively lower than that on PAA (Supplemental Fig. 2). Increasing ligand density on PAA gels to levels higher than that quantified on HA by nearly 40% (Supplemental Fig. 2), did not affect cell spreading on soft PAA gels. Despite these differences in fibronectin coverage between HA and PAA cell spread area was higher on HA even at Fn concentrations of 10μg/ml (nearly 10 fold lower than Fn concentration on PAA) (Fig. 2A). Taken together, these results indicate that the observed differences in cell spreading between HA and PAA gels are not due to greater ligand availability on the HA hydrogel system. Cells continue to respond to relative stiffness changes of HA based gels, indicating that the mechanical dependence of cell spreading is not entirely abrogated (Fig. 2B).

The spreading rate of mouse embryonic fibroblasts (MEFs) was monitored on varying Fn-coated gels and Fn-coated glass. MEFs showed a rapid (within 2 minutes) spreading response on HA-Fn, an order of magnitude greater than that observed on Fn-coated PAA gels of the same elastic modulus and on high density Fn-coated glass (Fig. 2C). The almost

immediate response of MEFs to HA-Fn gels implies that the spreading of cells on these soft substrates does not require expression of new proteins that enable spreading of soft substrates, but rather is due to acute signals initiated by simultaneous engagement of HA and integrin ligands. The rapidity of the response and the spreading rate also make it highly unlikely that the cell remodels the substrate to stiffen its interface prior to spreading.

3.3. Cell spreading on arginine-glycine-aspartic acid (RGD) containing ligands

When collagen I (Col-I) was substituted for Fn as the integrin ligand, the enhanced spreading of MSCs, seen on HA-Fn gels (Fig. 3A), was not observed consistent with other reports [44]. Similarly an attenuated cell spreading response was observed when the HA gels were functionalized with poly-L-lysine or N-cadherin (Fig. 3A). However, HA gels functionalized with the RGD-containing integrin ligand laminin facilitated spreading of hMSCs nearly as well as Fn (Fig. 3A).

In order to test whether HA and the integrin ligand need to be in close proximity to elicit the spreading of MSCs on soft PAA gels, cells were plated on 300 Pa PAA-Fn gels to engage integrins on their basal surface and then covered on their dorsal surface with HA, HA-Fn or HA-Col-I gels of similar stiffness (Fig. 3B). When HA or HA-Col-I gels were sandwiched on top of a soft (300Pa) PAA-Fn gel, the hMSCs did not spread (Fig. 3C). However, when Fn-incorporated HA gels were sandwiched on top of the PAA-Fn gels, the cells spread to an average area (2890 μm^2) that is 6 times greater than on PAA-Fn and 55% of that on 30 kPa PA-Fn or 40% of the area on HA-Fn alone (Fig. 3C). These results further support the above findings that biochemical signals activated by HA and its receptors require a proximal interplay with RGD specific integrin adhesion receptors. When cells were cultured on 300 Pa PAA-Col-I substrates, application of HA alone on their dorsal surface had no effect, but HA-Fn gels caused them to detach from the PAA-Col-I substrates (data not shown).

To test for the possibility that the effect of HA in the matrix depended on its potential to bind Fn or laminin and change their effects on integrins, RGD peptides were tethered directly to the HA scaffolds without additional intact proteins. RGD-HA gels also enabled myocyte and cardiac fibroblast spreading, comparable to Fn-HA (Fig. 4 A, B). Myocytes were also able to spread on Col-IV, although not to the same magnitude as that observed on Fn or RGD (Fig. 4B). However spreading on Col-IV (~800μm^2) was higher than on Fn coated PAA gels of similar stiffness (~500μm^2). Accumulatively, these results support the findings that the enhanced spreading of the mesenchymal cells studied here on HA is specific to RGD containing ECM ligands.

3.4. Cell proliferation on soft HA and PAA-Fn hydrogels

MSCs (Fib. 5A), fibroblasts (Fig. 5B), and endothelial cells (HUVEC) (Fig. 5C) cultured on 300Pa HA-Fn gels showed increased proliferation, overcoming the previously described cell-cycle block associated with very soft substrates [8, 38] (Fig. 5). Similarly to spreading, cell proliferation requires the combination of HA and Fn and does not occur on HA alone or on HA-Col-I, which allows initial adhesion but neither proliferation nor long term survival (Fig. 5).

3.5. Atomic force microscopy measurements of cell and gel stiffness

The mechanism by which cells are able to spread on HA-Fn gels could be due either to increase acto-myosin contractility and cortical stiffening normally activated by rigid substrates, by stiffening of the HA-Fn gel due to secretion of factors from the cell, or by different structural changes such as lowering cortical tension to allow increased adhesion to the surface. In order to determine whether cell stiffened the matrix underneath them, the

Young's modulus of the same spot of an HA-Fn gel was measured by atomic force microscopy before and after 24 hours of cell adhesion/spreading.

Storage moduli of hydrogels determined by AFM were consistent with our previous measurement by microscopy rheological, methods [12], showing shear modulus values below G'~500 Pa (Fig. 6A). Only a slight but not statistically significant increase in shear modulus of HA-Fn gels was observed when compared to HA alone or HA-collagen I gels (Fig. 6A). The elastic modulus of 3T3 fibroblasts spread on HA-Fn, as determined by AFM, was less than half than that of cells spread to the same extent on Fn-coated glass (Fig. 6 B, C). To determine whether the observed spreading results from the ability of the cells to increase the stiffness of the gel beneath the cell, 3T3 fibroblasts were detached from HA-Fn gels and the stiffness of the gel beneath the cell was measured. As shown in Figure 6 (D, E), 3T3 fibroblasts have an elastic modulus similar to that of the HA-Fn gel in close proximity to their cell edge. Measurement of the HA-Fn gel at the cell adhesion site immediately after removing the cell revealed an elastic modulus similar to that of the spread cell and the areas of the gel to which no cells were attached (Fig. 6E).

3.6. Traction forces on 2D and in 3D HA-Fn gels

The low elastic modulus of HA-Fn gels does not necessarily mean that adherent cells cannot generate large traction forces, since the stress is approximately the product of the elastic modulus of the gel and the strain produced by the cell. To measure local strains, grid of arrays of 1 μm diameter fluorescent Fn dots were stamped onto HA gels (Fig. 7A), taking advantage of the sulfhydryl chemistry of the HA crosslinking reaction to covalently couple fluorescent Fn. Figure 7A shows that fibroblasts adhere to Fn-coated dots and form actin fibers, indistinguishable from stress fibers of cells plated on rigid substrates. The Fn dots undergo only small displacements associated with the low forces (Fig. 7A). The average displacement of the dot was 0.24 ±0.08 μm (n=3 cells; n=540dots/image), corresponding to a force of 0.15±0.05 nN and a stress of 190 Pa at each dot. The magnitude of the total force exerted by the cell was 45.72 ±7.94 nN (n=3 cell images), resulting in an average traction stress magnitude of 15±3 Pa.

In addition, stresses exerted by cardiac myocytes, measured by traction force microscopy using bead displacement on HA gels with continuous Fn coating was also only slightly higher than on soft PAA gels and much lower than on stiffer (5 kPa) gels (Fig. 7B), despite greater myocyte spreading and organized myofibrillar assembly on soft HA-Fn gels. Cardiac myocytes also exert low stresses when cultured within 3D gels formed by collagen, fibrin, and variable amounts of HA (Fig. 7C–E). Increasing HA within networks of collagen and fibrin fibers decreases the shear moduli of these cell-embedded gels (7D), and also decreases the degree to which cardiac myocytes compact them (7C). These changes were accompanied by increases in myocyte area (7E) consistent with the observed myocyte response on 2D HA-fibrinogen or HA-fibronectin surfaces (Fig. 1d).

3.7. YAP localization in cells on HA and PAA gels

Cell morphological (i.e., spreading, focal adhesion and stress fiber assembly) and proliferative changes seen on rigid substrates necessarily involve the nuclear localization of the transcriptional regulatory factors YAP/TAZ [45]. To test whether YAP/TAZ nuclear localization is required for the observed spreading and proliferation of cells on soft HA-Fn gels, immunostaining of cell spread on HA-Fn gels was compared to that of cells cultures of PAA-Fn gels with different rigidities. These studies confirmed that YAP progressively localizes to the nucleus in a stiffness-dependent manner on Fn-coated PAA (Fig. 8), but YAP remains exclusively cytoplasmic in well-spread cells on HA-Fn (Fig. 8). Therefore, the formation of adhesion sites and actin bundles on HA-Fn did not necessitate either the

rigidity-dependent signals that localize YAP/TAZ to the nucleus or the transcriptional changes triggered by YAP/TAZ.

4.0. Discussion

Most primary cell types cannot spread and assemble actin fibers on soft substrates, with the exception of neurons [46, 47]. This is because the resistance provided by soft substrate is too low for cells to develop the required acto-myosin generated force to assemble integrin clusters, a prerequisite for enhanced focal adhesion assembly which in turn regulates cell spreading and actin fiber assembly [48–50]. In contradistinction as shown in this study, on equivalently soft HA-based substrates that contained appropriate integrin ligands, myocytes, fibroblasts, HUVECs and mesenchymal stem cells formed prominent integrin clusters, large focal adhesion complexes and enhanced cell spreading, despite considerably lower traction forces. The HA based hydrogels used in this study approximate the stiffness of bone marrow, but are much softer than mature blood vessels, muscle, or connective tissue [51] from which these cell types were derived. The crosslinked HA gels used in this study are linearly elastic [12, 52] and hence the observed formation of stress fibers cannot be attributed to cell-mediated strain-stiffening due to contractile forces deforming the hydrogel matrix, as often occurs in semiflexible polymer gels made from fibrin or collagen I [53, 54]. It is conceivable that the thiol modification of hyaluronan to form the hydrogels can contribute to substrate stiffening over a period of days causing the cells to adapt to the rigidity of the underlying substrate [44]. However, the spreading rate of cells on HA gels was rapid (within 2 minutes) and much faster than the rate at which increased thiol activation occurs or at which cells could synthesize and secrete matrix components that might stiffen the substrates. Therefore, spreading and cytoskeletal assembly initiated by the combination of HA and Fn, occurs much faster than the possible substrate remodeling and/ or topological modification. In support of this finding, measuring the shear modulus of the gels before, after and during cell attachment did not reveal changes in substrate elasticity (Fig. 6E). Moreover, to prevent any possibility of continuous stiffening of HA gels, cysteine was added to cap the thiol groups, and this also did not materially affect the observed cell spreading (Supplemental Fig. 3). Taken together, these results suggest that modification of the underlying substrate elasticity is not a likely explanation for the observed spreading on soft HA-Fn gels.

HA matrices are often considered to be inert, because normal cells do not adhere to them unless an integrin ligand is also attached. Although many cancer cell types that express CD44 splice variants adhere directly to HA [55, 56], hyaluronan receptors alone do not mediate stable adhesion of most non-transformed cell types, including all the cell types tested here. When adhesive ligands such as fibronectin, collagen I, laminin, collagen IV and cadherin are incorporated into the HA gels, cells are able to form attachments. Adhesion ligands need to be incorporated into the HA, and no cell attachment was observed if the pre-formed HA gel was incubated with soluble Fn, collagen I, PLL, or N-cadherin.

Cell spreading accompanied by assembly of FA structures and actin fiber bundles was only observed for RGD containing ligands such as fibronectin, laminin [57] or collagen IV [58]. Collagen I has cryptic RGD binding sites which can be exposed by MMP cleavage of collagen fibrils [59]. However, myocytes and non-muscle cells do not spread on collagen I incorporated HA gels, implying that these cryptic RGD binding sites are not exposed when incorporated in HA gels. RGD peptide alone was sufficient for cardiac myocytes and fibroblasts to spread and assemble myofibrils or actin fibers. These findings argue against the possibility that cell spreading on HA hydrogels are a result of changes in fibronectin conformation that alter adhesion to integrins [60].

MSCs, fibroblasts, and endothelial cells (HUVEC) (Fig. 5) proliferated after being plated on 300 Pa HA-Fn, a stiffness at which they are quiescent when cultured on PAA-Fn gels [38]. Remarkably, the proliferation was specific to fibronectin-containing HA hydrogels, whereas collagen I or HA alone were not capable to elicit a similar response. These results further support the findings that cell spreading and FA assembly are specific to RGD containing ligands in combination with HA.

Although the crosslinking chemistry for all incorporated ECM ligands in HA hydrogels was similar, cell spreading, proliferation was not universal and was specific to RGD alone or RGD containing ligands. Importantly, incorporation of different ECM ligands did not significantly affect the mechanical properties of the substrate (Fig. 6A), ruling out the possibility of crosslinking chemistry being a possible explanation for the observed spreading on the soft HA gels. This result serves as added evidence (Fig. 6E) that the ability of cells to spread on HA-Fn gels cannot be explained by increases in stiffness of the gel beneath the cell.

Numerous studies have established that the physical properties of cells such as contractility and cortical cell stiffness increase with stress fiber and FA assembly in spread cells as a function of substrate rigidity [14, 24, 61–64]. This study shows that despite similar spread areas of cells on HA-Fn gels and rigid substrates, the internal cell stiffness of cells on HA is nearly 50% lower than that measured on glass. Traction stresses exerted by fibroblasts and muscle cells were found to be low despite large spread areas consistent with a lower degree of internal tension. The computed stress values of 15 Pa are similar to that reported for poorly spread, muscle and non-muscle cells on relatively soft (1 kPa) PAA gels [14, 65]. Cardiac myocytes and supporting cells also exerted low stresses and displayed higher spreading when cultured within 3D gels formed by collagen, fibrin, and variable amounts of high molecular weight HA, consistent with the spreading observed on the sandwich 3D like constructs. The observed increase in cell spreading and stress fiber assembly on soft HA gels are not accompanied by high internal cell stiffness.

Recent studies have shown that the effectors of the hippo pathway, YAP/TAZ, are important transcriptional regulators involved in rigidity sensing and mechanotransduction [66]. The localization of YAP/TAZ in the nucleus has been reported to be directly involved in the cell spreading [45] and proliferation [67–69] response. The results from this study show that, similar to the original finding with epithelial cells [45], increasing the substrate rigidity on PAA-Fn gels causes YAP to localize in the nucleus in fibroblasts. Despite the enhanced cell proliferation and cell size on soft HA-Fn hydrogels, YAP did not localize in the nucleus, implying that the signaling pathways mediating rigidity sensing and spreading on HA-Fn substrates are not the same.

The findings from this study suggest the likely involvement of HA receptors along with RGD specific integrin adhesions, mediating the augmented cell phenotypic response as observed on soft HA hydrogels. The best characterized receptors of HA namely CD44 and CD168 or receptor for hyaluronan mediated motility (RHAMM) have been implicated in cellular processes such as motility associated with dynamic cytoskeletal changes [70]. RHAMM has the ability to bind and phosphorylate non-receptor tyrosine kinase Src [71], focal adhesion kinase [72] and erk kinase[73]. These signaling proteins are also engaged in the mechanosensory processes of cells when plated on substrates of varying rigidity [15]. Accordingly, it can be speculated that RHAMM activation by HA can lead to the phosphorylation of non-receptor tyrosine kinases, in a force-independent manner, capable of eliciting a cellular response similar to what is observed on stiff substrates. In addition, CD44 can directly interact with important cytoskeleton regulators like RhoA, a member of the Rho family of GTPases which control cell contractility and in turn actin filament organization

[74]. The specificity of cell proliferation and spreading to RGD ligands on soft HA gels suggest that there is an interplay between HA receptors and RGD specific integrins such as α5β1 and αvβ3. In support of this proposed mechanism, recent studies have suggested that there is a direct interplay between RGD specific integrins and RHAMM [75]. Future studies will therefore be necessary to examine the interplay between these receptors and their downstream biochemical signals that may be intimately involved in overriding the rigidity sensing response of cells residing in a hyaluronan enriched extracellular milieu.

5.0. Conclusion

The magnitude of forces and stiffnesses that elicit specific cellular responses and the molecular mechanisms by which cells transmit forces or transduce them into chemical or electrical signals are incompletely known, and are likely to depend on simultaneous chemical stimulation and other microenvironment inputs. The fact that HA production is tightly regulated during development and injury and frequently up-regulated in cancers characterized by uncontrolled growth and cell movement suggests that the interaction of signaling between HA receptors and specific integrins might be an important element in mechanical control of development and homeostasis. The results from this study show that the mechanosensitivity of a cell depends on the biochemical composition of its microenvironment even when the ligands that alter mechanosensitivity, such as HA, are not the primary adhesion receptors. These studies offer a new paradigm for understanding the biochemical and mechanical cooperative signaling emanating from the extracellular matrix. The integration of HA with integrin-specific ECM signaling proteins provides a rationale for engineering a new class of soft hybrid hydrogels that can be used in therapeutic/ tissue engineering strategies.

Supplementary Material

Refer to Web version on PubMed Central for supplementary material.

References

1. Levental I, Levental KR, Klein EA, Assoian R, Miller RT, Wells RG, et al. A simple indentation device for measuring micrometer-scale tissue stiffness. J Phys Condens Matter. 2010; 22:194120. [PubMed: 21386443]

2. Wells RG, Discher DE. Matrix elasticity, cytoskeletal tension, and TGF-beta: the insoluble and soluble meet. Sci Signal. 2008; 1:pe13. [PubMed: 18334714]

3. Kothapalli D, Liu SL, Bae YH, Monslow J, Xu T, Hawthorne EA, et al. Cardiovascular protection by ApoE and ApoE-HDL linked to suppression of ECM gene expression and arterial stiffening. Cell Rep. 2012; 2:1259–1271. [PubMed: 23103162]

4. Georges PC, Hui JJ, Gombos Z, McCormick ME, Wang AY, Uemura M, et al. Increased stiffness of the rat liver precedes matrix deposition: implications for fibrosis. Am J Physiol Gastrointest Liver Physiol. 2007; 293:G1147–1154. [PubMed: 17932231]

5. Perepelyuk M, Terajima M, Wang AY, Georges PC, Janmey PA, Yamauchi M, et al. Hepatic stellate cells and portal fibroblasts are the major cellular sources of collagens and lysyl oxidases in normal liver and early after injury. Am J Physiol Gastrointest Liver Physiol. 2013; 304:G605–614. [PubMed: 23328207]

6. Olsen AL, Bloomer SA, Chan EP, Gaca MD, Georges PC, Sackey B, et al. Hepatic stellate cells require a stiff environment for myofibroblastic differentiation. Am J Physiol Gastrointest Liver Physiol. 2011; 301:G110–118. [PubMed: 21527725]

7. Li Z, Dranoff JA, Chan EP, Uemura M, Sevigny J, Wells RG. Transforming growth factor-beta and substrate stiffness regulate portal fibroblast activation in culture. Hepatology. 2007; 46:1246–1256. [PubMed: 17625791]

8. Klein EA, Yin L, Kothapalli D, Castagnino P, Byfield FJ, Xu T, et al. Cell-cycle control by physiological matrix elasticity and in vivo tissue stiffening. Curr Biol. 2009; 19:1511–1518. [PubMed: 19765988]

9. Schrader J, Gordon-Walker TT, Aucott RL, van Deemter M, Quaas A, Walsh S, et al. Matrix stiffness modulates proliferation, chemotherapeutic response, and dormancy in hepatocellular carcinoma cells. Hepatology. 2011; 53:1192–1205. [PubMed: 21442631]

10. Pelham RJ Jr, Wang Y. Cell locomotion and focal adhesions are regulated by substrate flexibility. Proc Natl Acad Sci U S A. 1997; 94:13661–13665. [PubMed: 9391082]

11. Byfield FJ, Wen Q, Leventhal I, Nordstrom K, Arratia PE, Miller RT, et al. Absence of filamin A prevents cells from responding to stiffness gradients on gels coated with collagen but not fibronectin. Biophys J. 2009; 96:5095–5102. [PubMed: 19527669]

12. Chopra A, Lin V, McCollough A, Atzet S, Prestwich GD, Wechsler AS, et al. Reprogramming cardiomyocyte mechanosensing by crosstalk between integrins and hyaluronic acid receptors. J Biomech. 2012; 45:824–831. [PubMed: 22196970]

13. Ganz A, Lambert M, Saez A, Silberzan P, Buguin A, Mege RM, et al. Traction forces exerted through N-cadherin contacts. Biol Cell. 2006; 98:721–730. [PubMed: 16895521]

14. Chopra A, Tabdanov E, Patel H, Janmey PA, Kresh JY. Cardiac myocyte remodeling mediated by N-cadherin-dependent mechanosensing. Am J Physiol Heart Circ Physiol. 2011; 300:H1252–1266. [PubMed: 21257918]

15. Discher DE, Janmey P, Wang YL. Tissue cells feel and respond to the stiffness of their substrate. Science. 2005; 310:1139–1143. [PubMed: 16293750]

16. Giannone G, Sheetz MP. Substrate rigidity and force define form through tyrosine phosphatase and kinase pathways. Trends Cell Biol. 2006; 16:213–223. [PubMed: 16529933]

17. Bischofs IB, Safran SA, Schwarz US. Elastic interactions of active cells with soft materials. Phys Rev E Stat Nonlin Soft Matter Phys. 2004; 69:021911. [PubMed: 14995495]

18. Wipff PJ, Rifkin DB, Meister JJ, Hinz B. Myofibroblast contraction activates latent TGF-beta1 from the extracellular matrix. J Cell Biol. 2007; 179:1311–1323. [PubMed: 18086923]

19. Ju YE, Janmey PA, McCormick ME, Sawyer ES, Flanagan LA. Enhanced neurite growth from mammalian neurons in three-dimensional salmon fibrin gels. Biomaterials. 2007; 28:2097–2108. [PubMed: 17258313]

20. Georges PC, Miller WJ, Meaney DF, Sawyer ES, Janmey PA. Matrices with compliance comparable to that of brain tissue select neuronal over glial growth in mixed cortical cultures. Biophys J. 2006; 90:3012–3018. [PubMed: 16461391]

21. Kostic A, Sap J, Sheetz MP. RPTPalpha is required for rigidity-dependent inhibition of extension and differentiation of hippocampal neurons. J Cell Sci. 2007; 120:3895–3904. [PubMed: 17940065]

22. Zhang S, Sun A, Liang Y, Chen Q, Zhang C, Wang K, et al. A role of myocardial stiffness in cell-based cardiac repair: a hypothesis. J Cell Mol Med. 2009; 13:660–663. [PubMed: 19243474]

23. Berry MF, Engler AJ, Woo YJ, Pirolli TJ, Bish LT, Jayasankar V, et al. Mesenchymal stem cell injection after myocardial infarction improves myocardial compliance. Am J Physiol Heart Circ Physiol. 2006; 290:H2196–2203. [PubMed: 16473959]

24. Engler AJ, Carag-Krieger C, Johnson CP, Raab M, Tang HY, Speicher DW, et al. Embryonic cardiomyocytes beat best on a matrix with heart-like elasticity: scar-like rigidity inhibits beating. J Cell Sci. 2008; 121:3794–3802. [PubMed: 18957515]

25. Kresh JY, Chopra A. Intercellular and extracellular mechanotransduction in cardiac myocytes. Pflugers Arch. 2011; 462:75–87. [PubMed: 21437600]

26. Zamir EA, Taber LA. Material properties and residual stress in the stage 12 chick heart during cardiac looping. J Biomech Eng. 2004; 126:823–830. [PubMed: 15796341]

27. Yao J, Varner VD, Brilli LL, Young JM, Taber LA, Perucchio R. Viscoelastic material properties of the myocardium and cardiac jelly in the looping chick heart. J Biomech Eng. 2012; 134:024502. [PubMed: 22482677]

28. Lesley J, Hyman R, Kincade PW, Frank JD. CD44 and Its Interaction with Extracellular Matrix. Adv Immunol. 1993:271–335. [PubMed: 8379464]

29. Turley EA, Austen L, Vandeligt K, Clary C. Hyaluronan and a cell-associated hyaluronan binding protein regulate the locomotion of ras-transformed cells. J Cell Biol. 1991; 112:1041–1047. [PubMed: 1705559]

30. Borowsky ML, Hynes RO. Layilin, a novel talin-binding transmembrane protein homologous with C-type lectins, is localized in membrane ruffles. J Cell Biol. 1998; 143:429–442. [PubMed: 9786953]

31. McCourt PA, Ek B, Forsberg N, Gustafson S. Intercellular adhesion molecule-1 is a cell surface receptor for hyaluronan. J Biol Chem. 1994; 269:30081–30084. [PubMed: 7527024]

32. Isemura M, Yosizawa Z, Koide T, Ono T. Interaction of fibronectin and its proteolytic fragments with hyaluronic acid. J Biochem. 1982; 91:731–734. [PubMed: 7068586]

33. McDevitt CA, Marcelino J, Tucker L. Interaction of intact type VI collagen with hyaluronan. FEBS Lett. 1991; 294:167–170. [PubMed: 1756855]

34. Heldin P, Pertoft H. Synthesis and assembly of the hyaluronan-containing coats around normal human mesothelial cells. Exp Cell Res. 1993; 208:422–429. [PubMed: 8375471]

35. Rooney P, Kumar S. Inverse relationship between hyaluronan and collagens in development and angiogenesis. Differentiation. 1993; 54:1–9. [PubMed: 7691668]

36. Longaker MT, Chiu ES, Adzick NS, Stern M, Harrison MR, Stern R. Studies in fetal wound healing. V. A prolonged presence of hyaluronic acid characterizes fetal wound fluid. Ann Surg. 1991; 213:292–296. [PubMed: 2009010]

37. Burdick JA, Prestwich GD. Hyaluronic Acid Hydrogels for Biomedical Applications. Adv Mater. 2011

38. Winer JP, Janmey PA, McCormick ME, Funaki M. Bone marrow-derived human mesenchymal stem cells become quiescent on soft substrates but remain responsive to chemical or mechanical stimuli. Tissue Eng Part A. 2009; 15:147–154. [PubMed: 18673086]

39. Tseng Q, Duchemin-Pelletier E, Deshiere A, Balland M, Guillou H, Filhol O, et al. Spatial organization of the extracellular matrix regulates cell-cell junction positioning. Proc Natl Acad Sci U S A. 2012; 109:1506–1511. [PubMed: 22307605]

40. Tseng Q, Wang I, Duchemin-Pelletier E, Azioune A, Carpi N, Gao J, et al. A new micropatterning method of soft substrates reveals that different tumorigenic signals can promote or reduce cell contraction levels. Lab Chip. 2011; 11:2231–2240. [PubMed: 21523273]

41. Yang MT, Fu J, Wang YK, Desai RA, Chen CS. Assaying stem cell mechanobiology on microfabricated elastomeric substrates with geometrically modulated rigidity. Nat Protoc. 2011; 6:187–213. [PubMed: 21293460]

42. Polio SR, Rothenberg KE, Stamenovic D, Smith ML. A micropatterning and image processing approach to simplify measurement of cellular traction forces. Acta Biomater. 2012; 8:82–88. [PubMed: 21884832]

43. Friedland JC, Lee MH, Boettiger D. Mechanically activated integrin switch controls alpha5beta1 function. Science. 2009; 323:642–644. [PubMed: 19179533]

44. Rehfeldt F, Brown AE, Raab M, Cai S, Zajac AL, Zemel A, et al. Hyaluronic acid matrices show matrix stiffness in 2D and 3D dictates cytoskeletal order and myosin-II phosphorylation within stem cells. Integr Biol (Camb). 2012; 4:422–430. [PubMed: 22344328]

45. Dupont S, Morsut L, Aragona M, Enzo E, Giulitti S, Cordenonsi M, et al. Role of YAP/TAZ in mechanotransduction. Nature. 2011; 474:179–183. [PubMed: 21654799]

46. Yeung T, Georges PC, Flanagan LA, Marg B, Ortiz M, Funaki M, et al. Effects of substrate stiffness on cell morphology, cytoskeletal structure, and adhesion. Cell Motil Cytoskeleton. 2005; 60:24–34. [PubMed: 15573414]

47. Georges PC, Janmey PA. Cell type-specific response to growth on soft materials. J Appl Physiol. 2005; 98:1547–1553. [PubMed: 15772065]

48. Rossier OM, Gauthier N, Biais N, Vonnegut W, Fardin MA, Avigan P, et al. Force generated by actomyosin contraction builds bridges between adhesive contacts. EMBO J. 2010; 29:1055–1068. [PubMed: 20150894]

49. Galbraith CG, Yamada KM, Sheetz MP. The relationship between force and focal complex development. J Cell Biol. 2002; 159:695–705. [PubMed: 12446745]

50. Yu CH, Law JBK, Suryana M, Low HY, Sheetz MP. Early integrin binding to Arg-Gly-Asp peptide activates actin polymerization and contractile movement that stimulates outward translocation. Proc Natl Acad Sci U S A. 2011; 108:20585–20590. [PubMed: 22139375]

51. Levental I, Georges PC, Janmey PA. Soft biological materials and their impact on cell function. Soft Matter. 2007; 1:299–306.

52. Vanderhooft JL, Alcoutlabi M, Magda JJ, Prestwich GD. Rheological properties of cross-linked hyaluronan-gelatin hydrogels for tissue engineering. Macromol Biosci. 2009; 9:20–28. [PubMed: 18839402]

53. Storm C, Pastore JJ, MacKintosh FC, Lubensky TC, Janmey PA. Nonlinear elasticity in biological gels. Nature. 2005; 435:191–194. [PubMed: 15889088]

54. Winer JP, Oake S, Janmey PA. Non-linear elasticity of extracellular matrices enables contractile cells to communicate local position and orientation. PLoS One. 2009; 4:e6382. [PubMed: 19629190]

55. Welsh CF, Zhu D, Bourguignon LY. Interaction of CD44 variant isoforms with hyaluronic acid and the cytoskeleton in human prostate cancer cells. J Cell Physiol. 1995; 164:605–612. [PubMed: 7544357]

56. Ananthanarayanan B, Kim Y, Kumar S. Elucidating the mechanobiology of malignant brain tumors using a brain matrix-mimetic hyaluronic acid hydrogel platform. Biomaterials. 32:7913–7923. [PubMed: 21820737]

57. Tashiro K, Sephel GC, Greatorex D, Sasaki M, Shirashi N, Martin GR, et al. The RGD containing site of the mouse laminin A chain is active for cell attachment, spreading, migration and neurite outgrowth. J Cell Physiol. 1991; 146:451–459. [PubMed: 2022699]

58. Pedchenko V, Zent R, Hudson BG. alpha(v)beta(3) and alpha(v)beta(5) integrins bind both the proximal RGD site and non-RGD motifs within noncollagenous (NC1) domain of the alpha 3 chain of type IV collagen - Implication for the mechanism of endothelial cell adhesion. J Biol Chem. 2004; 279:2772–2780. [PubMed: 14610079]

59. Davis GE. Affinity of Integrins for Damaged Extracellular-Matrix - Alpha-V-Beta-3 Binds to Denatured Collagen Type-I through Rgd Sites. Biochem Biophys Res Commun. 1992; 182:1025–1031. [PubMed: 1540151]

60. Keselowsky BG, Collard DM, Garcia AJ. Surface chemistry modulates fibronectin conformation and directs integrin binding and specificity to control cell adhesion. J Biomed Mater Res A. 2003; 66:247–259. [PubMed: 12888994]

61. Solon J, Levental I, Sengupta K, Georges PC, Janmey PA. Fibroblast adaptation and stiffness matching to soft elastic substrates. Biophys J. 2007; 93:4453–4461. [PubMed: 18045965]

62. Tee SY, Fu J, Chen CS, Janmey PA. Cell shape and substrate rigidity both regulate cell stiffness. Biophys J. 2011; 100:L25–27. [PubMed: 21354386]

63. Kasza KE, Nakamura F, Hu S, Kollmannsberger P, Bonakdar N, Fabry B, et al. Filamin A is essential for active cell stiffening but not passive stiffening under external force. Biophys J. 2009; 96:4326–4335. [PubMed: 19450503]

64. Trichet L, Le Digabel J, Hawkins RJ, Vedula SR, Gupta M, Ribrault C, et al. Evidence of a large-scale mechanosensing mechanism for cellular adaptation to substrate stiffness. Proc Natl Acad Sci U S A. 2012; 109:6933–6938. [PubMed: 22509005]

65. Califano JP, Reinhart-King CA. Substrate Stiffness and Cell Area Predict Cellular Traction Stresses in Single Cells and Cells in Contact. Cell Mol Bioeng. 2010; 3:68–75. [PubMed: 21116436]

66. Halder G, Dupont S, Piccolo S. Transduction of mechanical and cytoskeletal cues by YAP and TAZ. Nat Rev Mol Cell Biol. 2012; 13:591–600. [PubMed: 22895435]

67. Xin M, Kim Y, Sutherland LB, Murakami M, Qi X, McAnally J, et al. Hippo pathway effector Yap promotes cardiac regeneration. Proc Natl Acad Sci U S A. 2013

68. Mendez MG, Janmey PA. Transcription factor regulation by mechanical stress. Int J Biochem Cell Biol. 2012; 44:728–732. [PubMed: 22387568]

69. Zhao B, Tumaneng K, Guan KL. The Hippo pathway in organ size control, tissue regeneration and stem cell self-renewal. Nat Cell Biol. 2011; 13:877–883. [PubMed: 21808241]

70. Turley EA, Noble PW, Bourguignon LY. Signaling properties of hyaluronan receptors. J Biol Chem. 2002; 277:4589–4592. [PubMed: 11717317]

71. Hall CL, Lange LA, Prober DA, Zhang S, Turley EA. pp60(c-src) is required for cell locomotion regulated by the hyaluronanreceptor RHAMM. Oncogene. 1996; 13:2213–2224. [PubMed: 8950989]

72. Hall CL, Wang C, Lange LA, Turley EA. Hyaluronan and the hyaluronan receptor RHAMM promote focal adhesion turnover and transient tyrosine kinase activity. J Cell Biol. 1994; 126:575–588. [PubMed: 7518470]

73. Hall CL, Yang B, Yang X, Zhang S, Turley M, Samuel S, et al. Overexpression of the hyaluronan receptor RHAMM is transforming and is also required for H-ras transformation. Cell. 1995; 82:19–26. [PubMed: 7541721]

74. Nobes CD, Hall A. Rho, rac, and cdc42 GTPases regulate the assembly of multimolecular focal complexes associated with actin stress fibers, lamellipodia, and filopodia. Cell. 1995; 81:53–62. [PubMed: 7536630]

75. Gares SL, Pilarski LM. Balancing thymocyte adhesion and motility: a functional linkage between beta1 integrins and the motility receptor RHAMM. Dev Immunol. 2000; 7:209–225. [PubMed: 11097213]
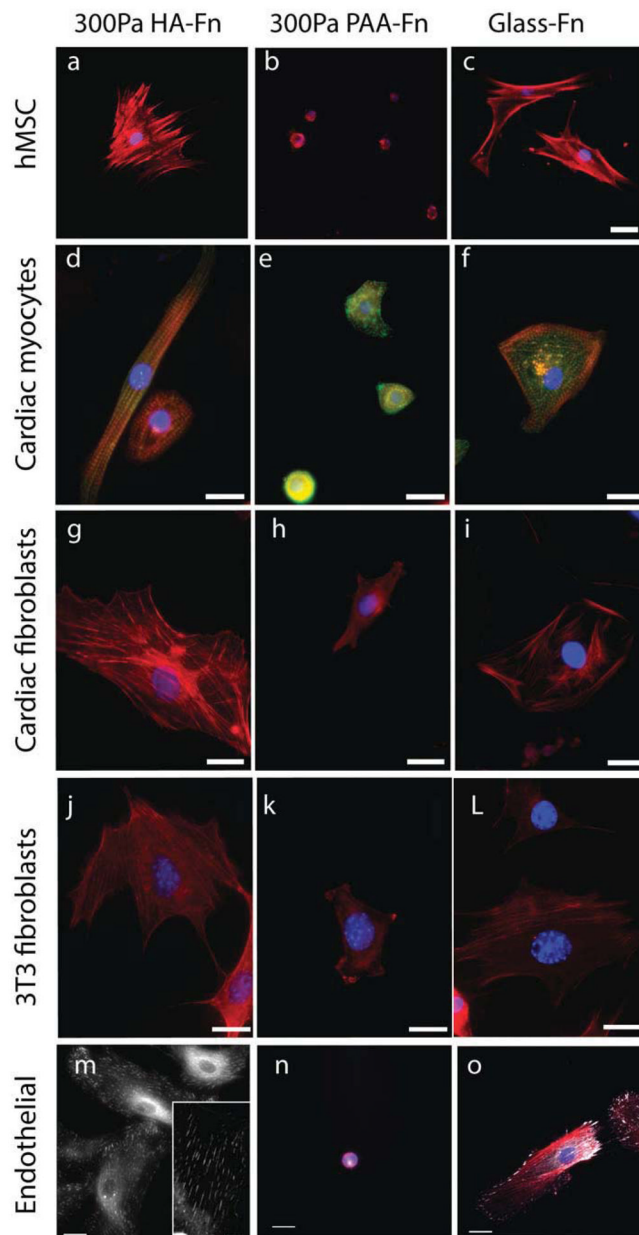
Figure 1. Development of stress fibers and focal adhesions on soft HA-Fn gels
Human mesenchymal stem cells (hMSCs), neonatal rat ventricular myocytes and fibroblasts, NIH 3T3 fibroblasts, and human umbilical vein endothelial cells (HUVECS) were plated on 300 Pa HA-fibronectin gels, 300 Pa PAA-fibronectin gels, or Fn-coated glass. Actin is stained with rhodamine-phalloidin (red) and cell nuclei are stained by DAPI (blue). Alpha actinin is stained green for myocytes, and paxillin is shown in white for endothelial cells. Scale bar represents 20μm.
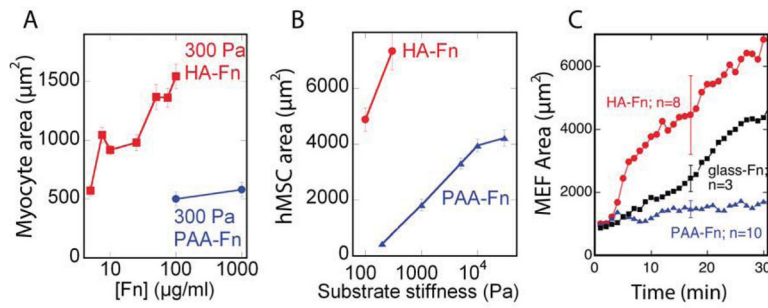
Figure 2. Enhanced cell spreading response on HA-fibronectin hydrogels
(A) Myocyte spread area on HA and PAA gels with identical shear modulus coated with varying amounts of Fn (n >100 cells). (B) MSC spread area on varying stiffnesses of polyacrylamide or HA gels coated with saturating amounts of Fn (n>100 cells). (C) Quantification of early fibroblast cell spread area over time on varying substrates (n>3). Error bars ±1 S.E..
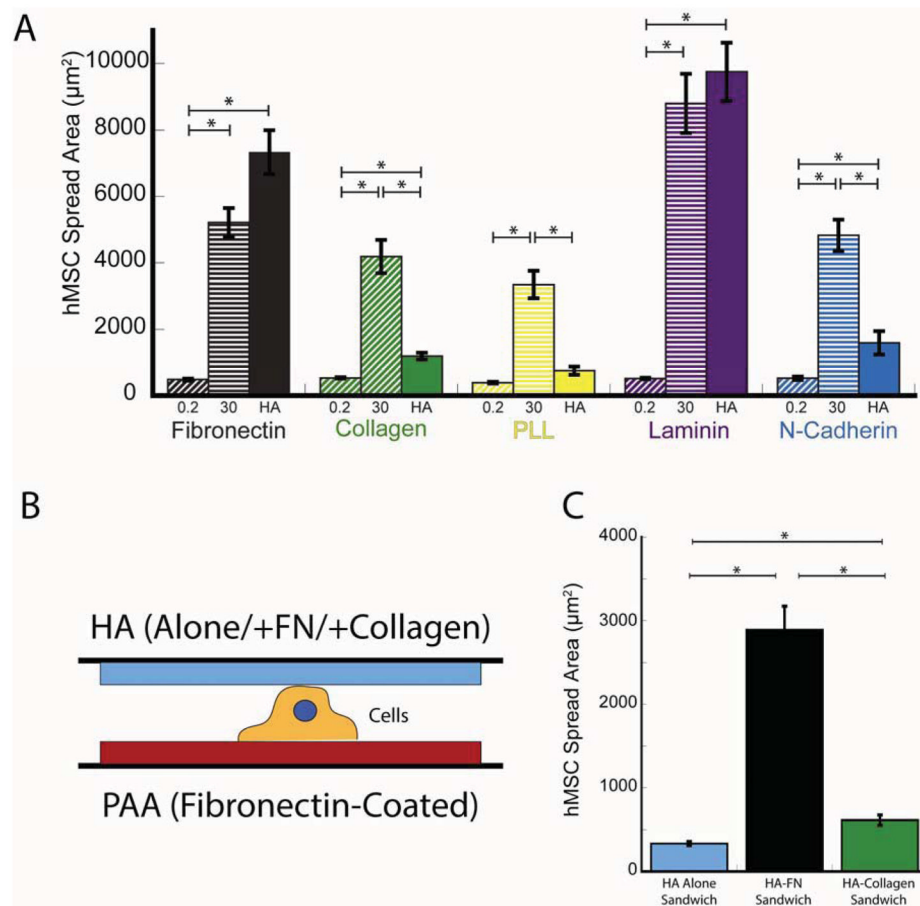
Figure 3. Cell spreading response as a function of ligand type
(A) Mesenchymal stem cell (MSC) spread area on different stiffness polyacrylamide or HA gels coated with saturating amounts of Fn, Collagen I, Poly-l-lysine (PLL), Laminin and N-cadherin. (B) Schematic representation of the sandwich construct, showing cells adhered to 300Pa PAA-Fn gels at the bottom with different HA-ligand compositions at the top. (C) MSC spread areas for cells sandwiched between 300Pa PAA-Fn and HA-alone/Fn/Col-I. *p<0.05, error bars ±1 SEM for n= 50 cells.
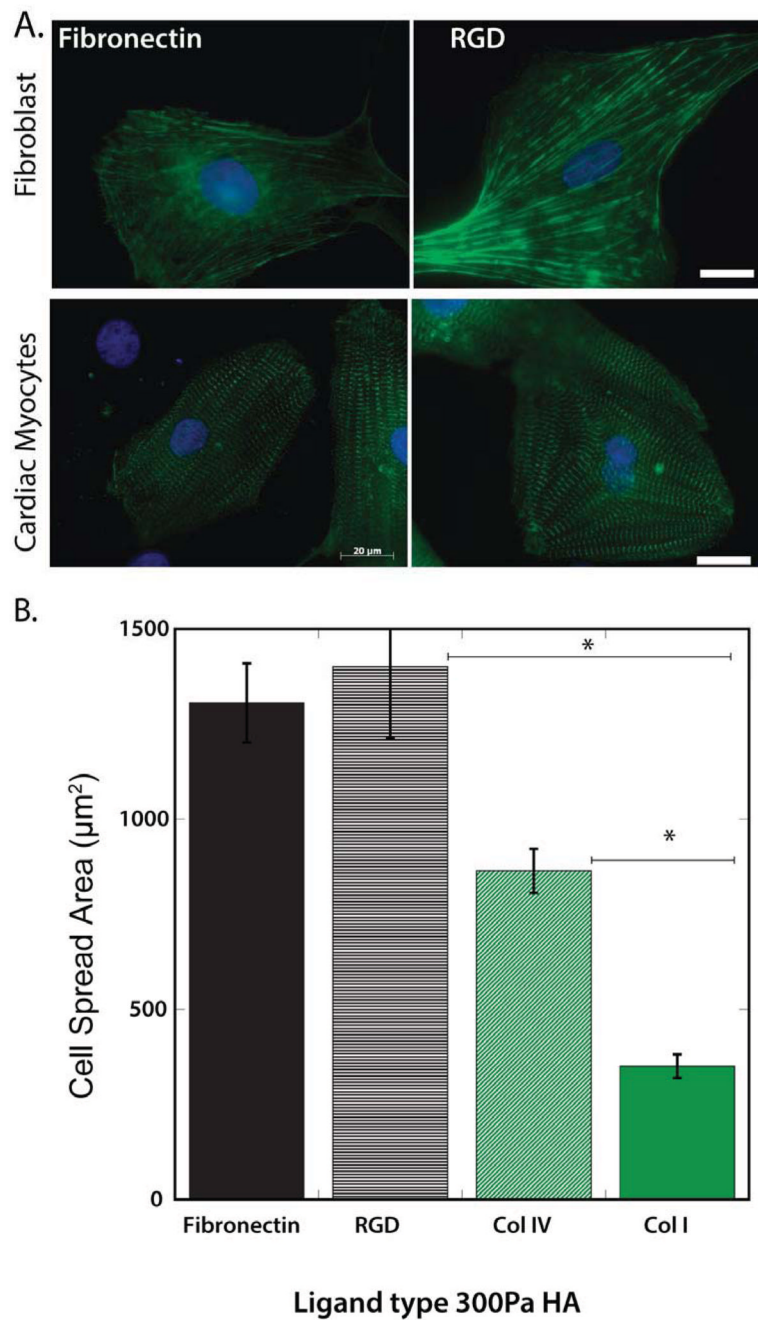
Figure 4. Cell spreading in response to HA incorporated with RGD alone or RGD containing ligands

(A) Cardiac fibroblasts and myocytes plated on HA-Fn and HA-RGD show comparable spread area, stress-fiber formation (f-actin; green) and myofibrillar assembly (α-actinin; green). (B) Spread area magnitudes of myocytes plated on fibronectin, RGD, collagen IV (Col IV) and I (Col I). *p<0.01, error bars ±1 SEM for n>100 cells.
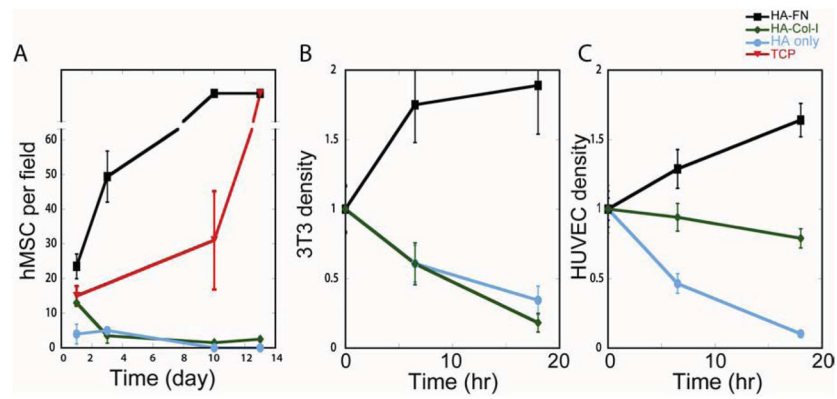
Figure 5. Enhanced cells proliferation on 300Pa HA-Fn gels
Proliferation rates of MSCs (A), fibroblasts (B) and HUVECs (C) on HA with or without different integrin ligands, and comparison of growth rates on PAA-Fn gels or tissue culture plastic (TCP). Error bars ±1 SEM for n>5 fields.
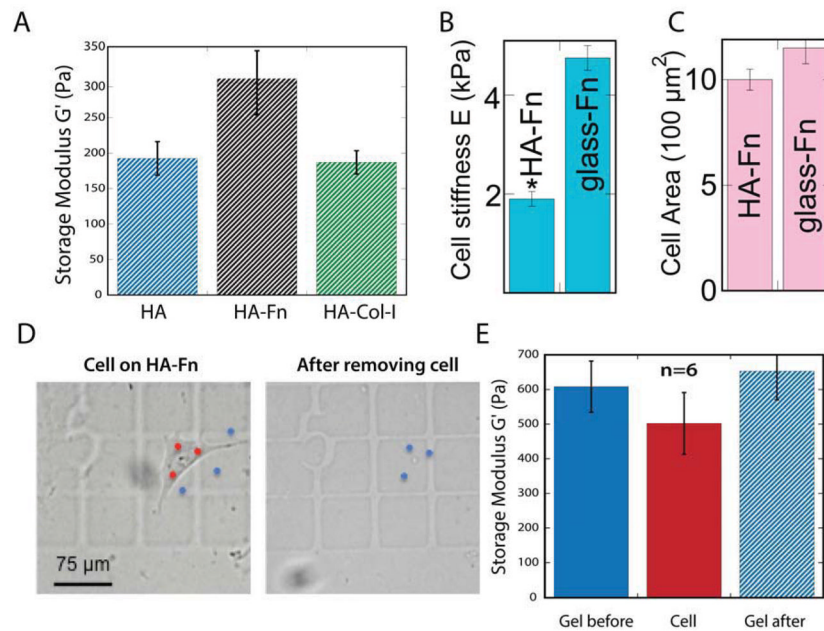
Figure 6. Cell and hydrogel material properties measured by atomic force microscopy
(A) Storage modulus of HA gels with different ECM ligands. (B, C) Comparison of cell stiffness and cell area on Fn coated HA and glass. (D) Left: image of a 3T3 fibroblast spread on an HA-FN gel prepared on top of a CELLocate coverslip. AFM was used to indent three areas of the cell (red dots) and three areas of the HA-Fn gel within 30 μm of the cell edge (blue dots). Right: HA-Fn gel shown in left image after cell has been detached. Blue dots indicate areas of the gel to which the cell had been previously attached that were indented by AFM. (E) Graph shows the measured elastic modulus of 3T3 fibroblasts attached to an HA-Fn gel, the HA-Fn gel in proximity of the attached cell and the area of the HA-Fn gel beneath the cell after cell detachment. No significant difference was observed between each set of measurements. *$p < 0.01$, error bars ±1 SEM for $n > 6$ cells; scale bar represents 75μm.
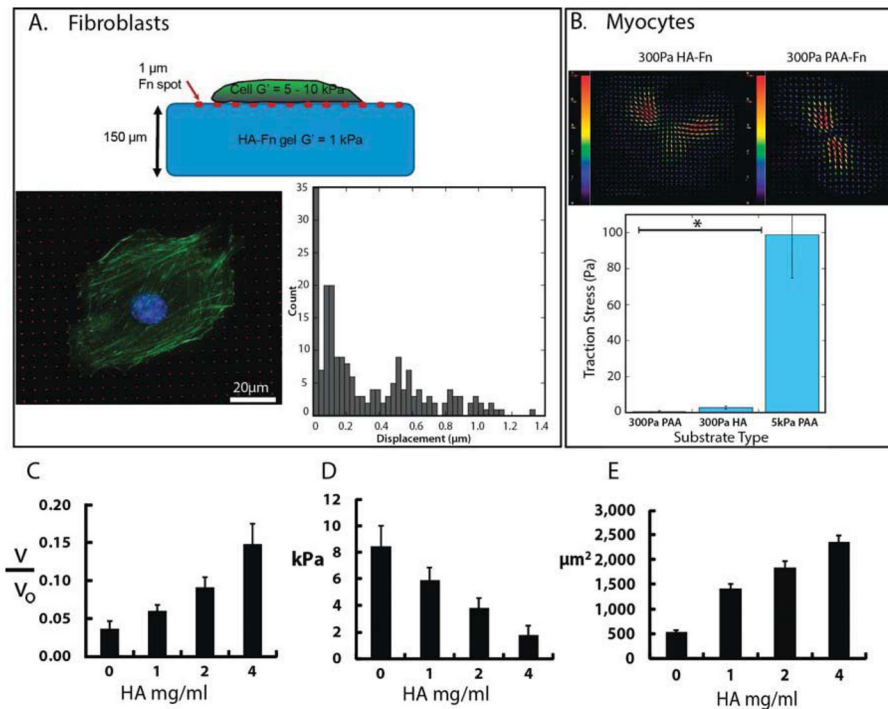
Figure 7. Cell traction forces exerted on 2D and within 3D hyaluronan gels
(A) Mouse embryonic fibroblasts were cultured on fibronectin micro-patterned dot grid
(1μm diameter) hyaluronan substrates. Traction stresses were estimated using the measured
displacement vectors of the Fn dot (n=3 cells). (B) Resting traction stresses of cardiac
myocytes calculated from the displacement of fluorescent beads incorporated in 300 Pa HA-
Fn or PAA-Fn gels. *$p<0.05$ error bars ±1 SEM for n>7 cells, scale bar indicates 20μm. (C)
cardiac cell mediated gel compaction n=10, (D) measured gel stiffness E (Young's modulus
for n=4) and (E) average area of myocytes with the compacted gels n=50, of constructs
formed by embedding cardiac myocytes and fibroblasts (10^6/ml) within gels composed of 1
mg/mL fibrin and 0.25 mg/mL collagen after 1 week. Error bars ±1 S.D.

A

Glass   HA-Fn

B
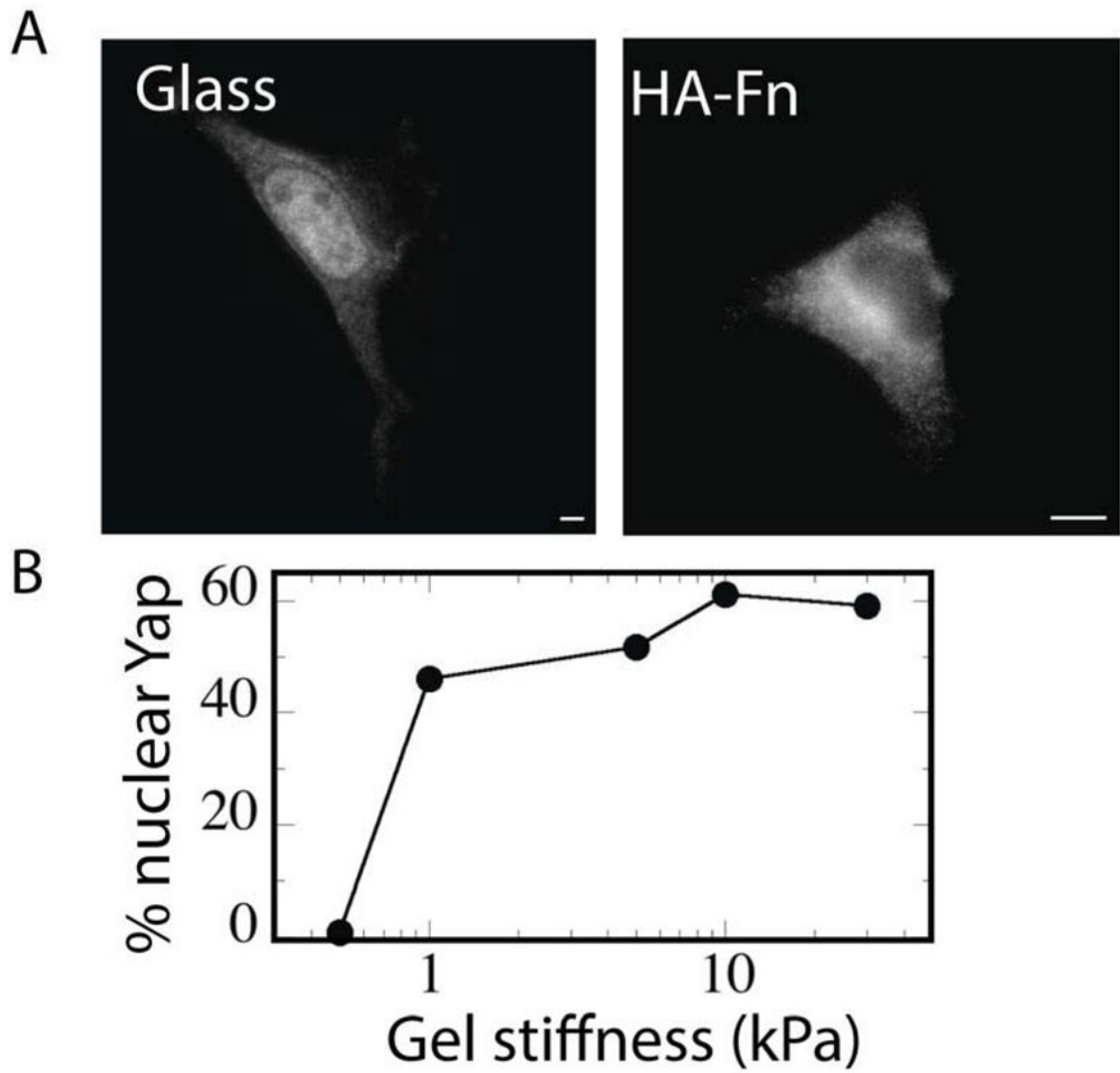
Figure 8. Measurement of YAP localization as a function of stiffness on PAA-fn and HA-Fn hydrogels
(A, B) Nuclear localization of Yap in fibroblasts with increasing stiffness on PAA-Fn, but not on HA-Fn (n= 250 cells from 3-different preparations).